Geomechanics and Engineering, *Vol. 33, No. 2 (2023) 167-174*
https://doi.org/10.12989/gae.2023.33.2.167

Application of UAV images for rainfall-induced slope stability analysis in urban areas

Dohyun Kim[1a], Junyoung Ko[2b] and Jaehong Kim*[3]

[1]*Department of Civil and Environmental Engineering, Hanbat National University, Daejeon 34158, South Korea*
[2]*Department of Civil Engineering, Chungnam National University, Daejeon 34134, South Korea*
[3]*Department of Civil and Environmental Engineering, Dongshin University, Naju, Jeonnam 58245, South Korea*

(*Received April 4, 2022, Revised July 3, 2022, Accepted August 12, 2022*)

Abstract. This study evaluated slope stability through a case study to determine the disaster risks associated with increased deforestation in structures, including schools and apartments, located in urban areas adjacent to slopes. The slope behind the OO High School in Gwangju, Korea, collapsed owing to heavy rain in August 2018. Historically, rainwater drained well around the slope during the rainy season. However, during the collapse, a large amount of seepage water flowed out of the slope surface and a shallow failure occurred along the saturated soil layer. To analyze the cause of the collapse, the images of the upper area of the slope, which could not be directly identified, were captured using unmanned aerial vehicles (UAVs). A digital elevation model of the slope was constructed through image analysis, making it possible to calculate the rainfall flow direction and the area, width, and length of logging areas. The change in the instability of the slope over time owing to rainfall lasting ten days before the collapse was analyzed through numerical analysis. Imaging techniques based on the UAV images were found to be effective in analyzing ground disaster risk maps in urban areas. Furthermore, the analysis was found to predict the failure before its actual occurrence.

Keywords: deforestation area; digital elevation model; slope failure; unmanned aerial vehicle; unsaturated soil

1. Introduction

Deforestation has continued to progress, with people remaining unaware of this trend because of the increase in convenience facilities, such as tourist facilities and walking trails in urban areas, implemented by local governments every year in addition to the increasing urbanization and industrialization in each region. This increase in deforestation is not only concentrated in road development projects but has also increased in urban areas adjacent to steep slopes, such as retaining walls and cut slopes. This phenomenon has become a key factor causing damage in the form of landslides. The probability of landslides resulting from deforestation significantly increases during the rainy season in Korea from June to August because of shallow slope failures and debris flow, and many human casualties and property damage suddenly occur (Peduto *et al.* 2021, Gulla *et al*. 2017).

In Korea, the geographic information system (GIS) technique has been used in research to analyze landslide disaster risk areas. The data collected from this research was used to produce a significant ground disaster risk map that can be used as basic data to ensure the safety of areas close to landslides and steep slope sites (MPSS 2012).

Previous studies on debris flow risks and landslides have focused on the technology required to determine the locations of slopes with a high landslide probability. This technology can identify the locations with high collapse probability in mountainous areas; however, its usability is limited because it cannot identify areas where damage is expected.

Latest technologies, such as unmanned aerial vehicles (UAVs), i.e., drones, have recently been used in areas with limited access to effectively cope with the risks associated with mountainous areas in cities. UAVs can perform measurements over wide areas, including hard-to-access areas. Moreover, UAVs can be introduced within a reasonable budget and provides a topographical survey technology operable by minimal personnel.

UAV-based surveys can provide high-resolution spatial information for the target area at the desired time in a rapid and cost-effective manner. In addition to the geometric information, they can acquire qualitative data, such as texture and color. Monitoring based on unmanned aerial photogrammetry is useful for quickly analyzing minute topographic changes in large-scale terrain.

Fig. 1 shows a drone image of the road collapse in Gokseong-gun, Jeolla-namdo caused by heavy rainfall. The depth calculation of the collapse site and soil quantity in three-dimensional coordinates obtained from the captured data is also included. In Korea, drones have been used to conduct research in various fields because two-dimensional area analysis through drone photogrammetry, slope analysis through digital elevation model (DEM), and landslide and collapse risk analysis are possible. UAVs (drones) can be

*Corresponding author, Professor
E-mail: woghd@dsu.ac.kr
[a]Professor
[b]Professor

Copyright © 2023 Techno-Press, Ltd.

ISSN: 2005-307X (Print), 2092-6219 (Online)

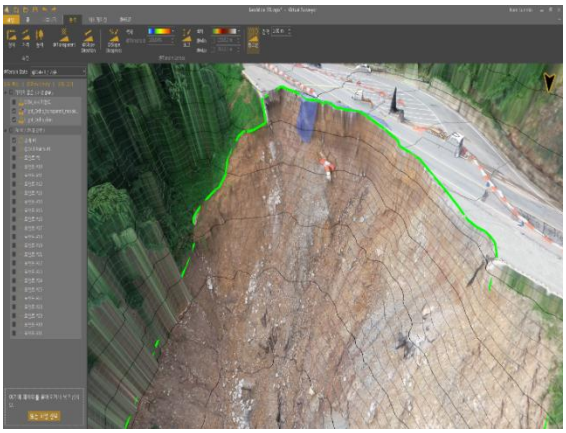

Fig. 1 Drone image of the road collapse caused by rainfall

Fig. 2 Location of failure in Gwangju, South Korea

effectively used for map production and disaster area analysis (Vasuki *et al*. 2014, Xiao *et al.* 2018). Therefore, in this study, drone images of a slope collapse site were analyzed and a slope failure stability evaluation was performed to verify the disaster risks of structures in urban areas, such as schools and apartment complexes, that are hard to access because of geotechnical constraints. Seepage analysis of unsaturated soils makes it possible to more efficiently determine the cause of shallow slope failures that frequently occur during the rainy season and offer preventive measures in advance (Kim *et al*. 2013).

2. Survey of the slope failure site in the logging area

2.1 Overview of the slope failure site

The target area for the UAV imaging was the slope near a high school, located in Gwangju, Korea. The slope behind the school building collapsed on August 31, 2018, owing to heavy rainfall. Rainwater had previously drained well by moving around the slope during the rainy season every year. However, during collapse, a large amount of seepage water flowed out of the slope surface, and the collapse occurred when excessive rainwater drained along the terrain surface.

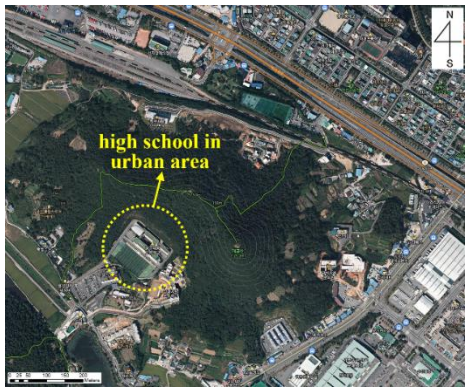

Fig. 3 Location of a high school and the adjacent area in Gwangju (UAV image)

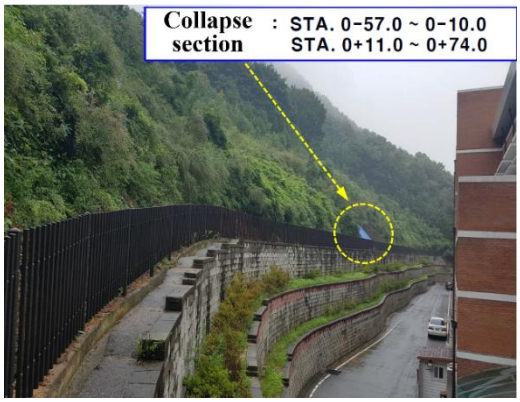

Fig. 4 Slope failure site behind the high school building

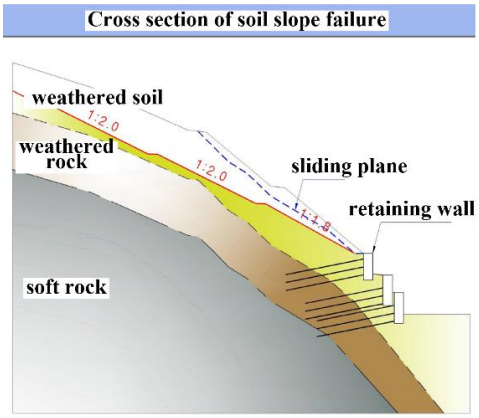

Fig. 4 Slope failure site behind the high school building

Fig. 6 Area surrounding the high school photographed by a UAV(Sept. 2015)

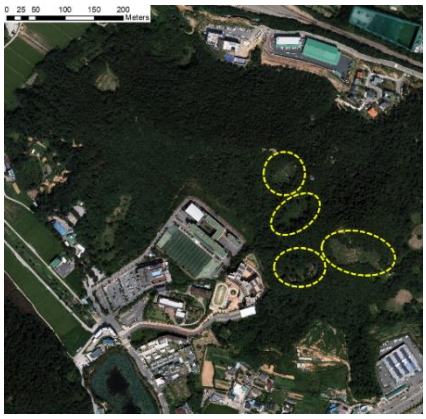

Fig. 7 Logging areas(yellow colors) photographed by a UAV (Sept. 2017)

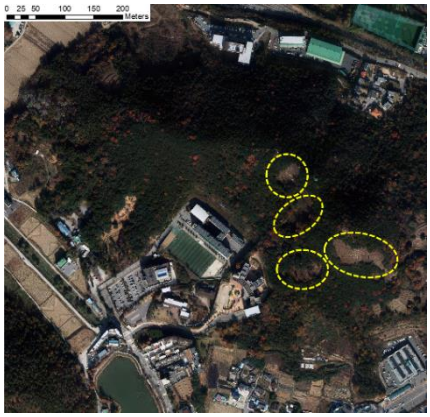

Fig. 8 Logging areas(yellow colors) photographed by a UAV (Nov. 2019)

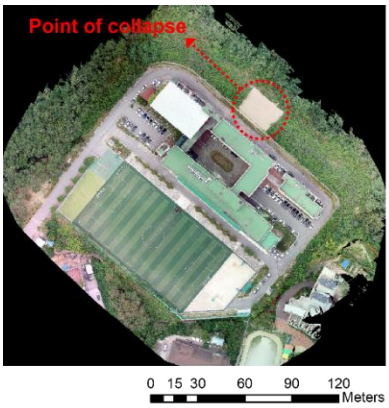

Fig. 9 Drone image of the collapsed slope in Gwangju

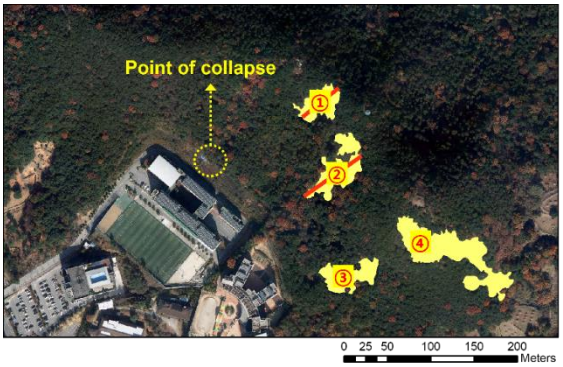

Fig. 10 Area and width of the logging area calculated by the photographic images

Fig. 3 shows a UAV image of the high school and the adjacent area in Gwangju where a slope failure occurred, and

Fig. 4 shows the location of the collapse of the retaining wall slope behind the high school building. The area covered by blue tarpaulin is the area where the collapse occurred (Fig. 4). The failure occurred in the soil layer; however, there was no damage to the retaining wall structure. Fig. 5 shows a cross-section of the slope reinforcement design. The site slope was steeper (1:1.7 to 1.4) than a standard slope (1:1.2 to 1.5), and many traces of scouring in the form of shallow failures owing to heavy rainfall were found.

2.2 Investigation of the cause of the slope failure using drone imaging

The slope behind the high school collapsed on August 31, 2018, due to heavy rainfall. However, as shown in Fig. 6, it has been a stable area without collapse every year, although it has rained a lot during the rainy season for more than a decade. Rainwater resulting from heavy rainfall was drained effectively near the retaining walls every year; however, a sudden slope failure occurred during the rainy season of 2018. Thus, images of the area surrounding the slope were captured using drones to determine the cause of slope failure. Based on these images, several areas in the upper regions of the slope, where bushes and trees had been logged, were identified. Figs. 6-8 can easily be found on general internet mapping sites. The aerial photographs, captured and recorded every two years, show that the logged sections existed in 2017, at least one year before the collapse. As seen in Fig. 7, the four slopes marked by yellow dotted lines show the areas where bushes and trees were logged compared to the same areas in 2015 (Fig. 6). Further logging areas can be seen from the image in 2019 (Fig. 8).

The slope of the retaining wall behind the school building acted as a stable civil engineering structure while water was drained yearly during the rainy season. However, the slope failure in August 2018 indicates significant rainfall infiltration in sections where the ground was exposed because of logging at least a year before the collapse, an increase in the groundwater level, and topographic changes caused by debris flow in the surface layer. A slope analysis was conducted through DEM using drone imaging data of the collapsed slope to further analyze the cause of the failure. Fig. 9 shows the drone image of the area behind the high school building where the collapse occurred from an altitude of 1,600 m. Fig. 10 shows the used by the software to calculate the area and width of the logging areas. The width was calculated as 54 and 81m for logging areas ① (closest to the collapsed slope) and ②, respectively (QGIS, 2020).

Fig. 11 shows the slope map derived from DEM. The slope directions are marked by different colors to identify

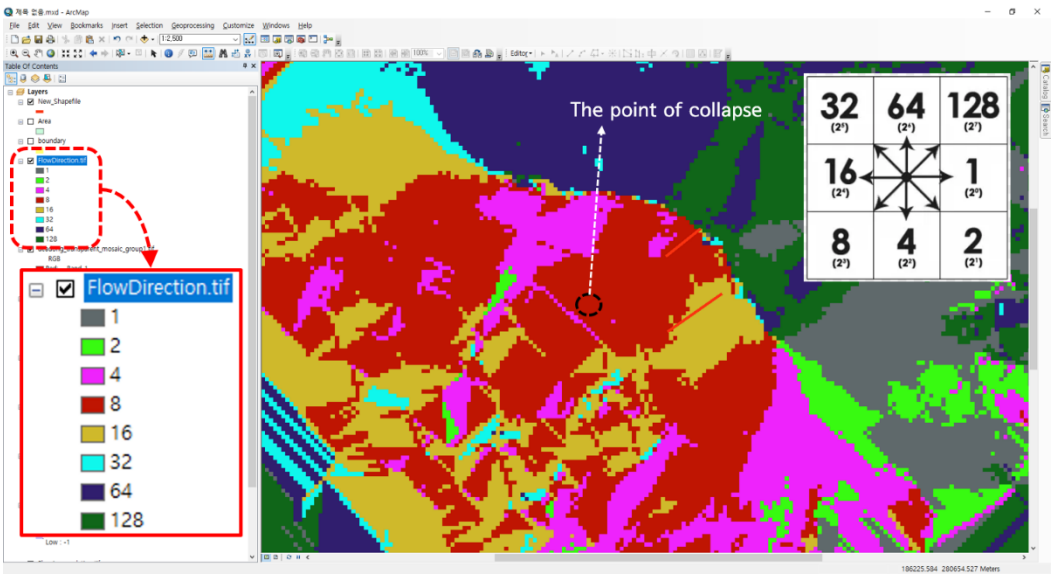

Fig. 11 DEM (slope map) for predicting the direction of water flow

Table 1 Strength and hydraulic properties of unsaturated soil

Soil Type	Unit weight (kN/m^3)	Cohesion (kPa)	Friction Angle (°)	a (kPa^{-1})	n	m	Permeability (m/s)
Weathered Soil	19.0	4.59	30	1.18	1.601	0.375	1.48×10^{-5}
Weathered Rock	20.0	30.0	30	10.0	1.601	0.375	5.68×10^{-7}
Soft Rock	23.0	50.0	35	30.0	1.601	0.375	1.05×10^{-8}

the water flow direction in the surface layer during rainfall. The width of the logging areas ① and ② shown in Fig. 10 are represented by straight red lines at the same positions in Fig. 11. The numbers give information on the area of logging, and when applying numerical analysis, the length of the logging area could be calculated in two dimensions.

The numbers and direction signs shown in the top right corner of Fig. 11 correspond to the directions by colors on the left. The rainwater can be predicted to flow along the surface layer in direction 8 (7 o'clock direction) for the section marked in red and direction 4 (6 o'clock direction) for the section marked in pink. For the slope section marked in yellow, the slope is formed in direction 16 (9 o'clock direction). These three slope directions confirm that the water flow is nearing the collapse point.

3. Unsaturated seepage and stability analyses according to rainfall analysis

A stability analysis was conducted for the retaining wall slope failure behind the high school building in Gwangju to identify the time of the collapse and the stages proceeding it by applying hourly rainfall data and conducting an unsaturated seepage analysis. Table 1 lists the physical properties of each stratum obtained through a geotechnical investigation at the time of the initial collapse. As shown in Fig. 5, the slope consisted of weathered soil, weathered rock, and bedrock.

To conduct unsaturated seepage analysis for each

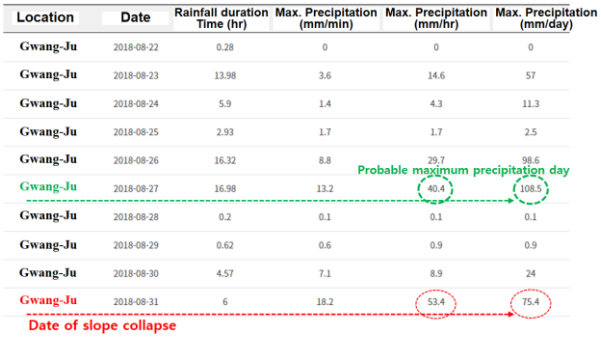

Fig. 12 Climate information for Gwangju (KMA 2018)

stratum and apply the experimental constants (a, n, m) of the soil–water characteristic curve, the average of the experimental values published in previous studies were applied (Al-Mahbashi *et al.* 2015, Kim *et al.* 2014, Kim *et al.* 2013, Kim *et al.* 2021). Table 1 lists the average values of the soil-water characteristic curve and saturated permeability coefficient by stratum used in the unsaturated seepage analysis.

Since the collapse occurred on August 31, 2018, the rainfall before this date is a factor causing instability of the slope. Fig. 12 shows the rainfall data for August 2018. These data can easily be obtained from the Korea Meteorological Administration (KMA) website (data.kma.go.kr). In Fig. 12, the section enclosed by a red dotted line represents the ten days before August 31, when the slope failure occurred. We confirmed continuous rainfall during this period, with the retaining wall slope collapsing

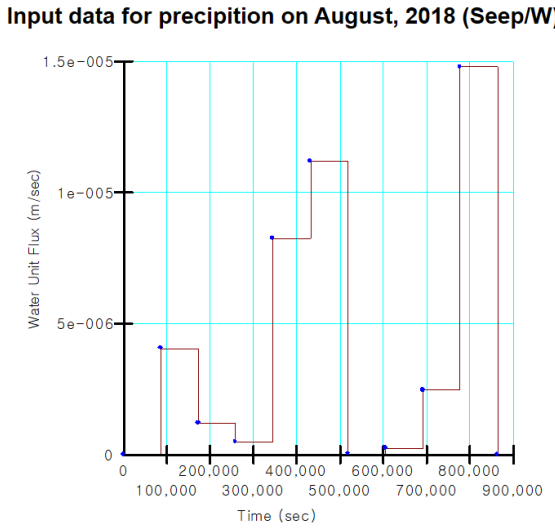

Fig. 13 Actual rainfall data for 10 days for seepage analysis

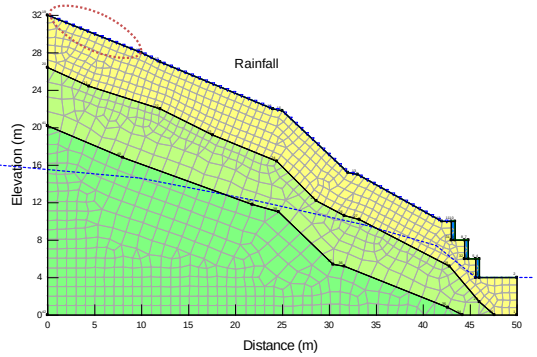

Fig. 14 Initial condition for unsaturated soil seepage analysis (SEEP/W)

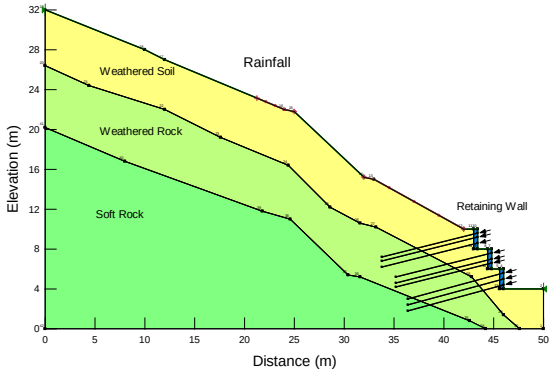

Fig. 15 Boundary condition for slope stability analysis (SLOPE/W)

on the last day (August 31). Fig. 13 shows the detailed daily rainfall for the ten days before the collapse. The maximum rainfall was recorded on the fifth day; however, the rainfall differed from that on August 31, when the collapse occurred. The maximum precipitation per day shown in Fig. 12 were applied as the seepage analysis rainfall conditions to conduct the slope stability analysis.

Fig. 13 shows the changes in rainfall data recorded in the actual August 2018 entered into the software. When

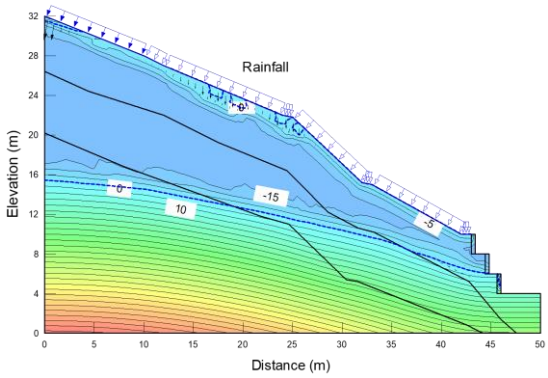

Fig. 16 Contour of pore water pressure (after 1 day)

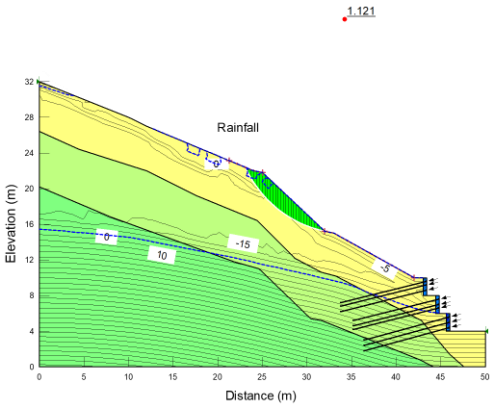

Fig. 17 Safety factor owing to 1 day of rainfall

86,400 seconds are calculated as 1 day, the final time shown in Fig. 13 shows the rainfall input data for 10 days (864,000 sec) (KMA Weather Data Service).

For the initial numerical analysis conditions with rainfall exceeding the permeability coefficient and occurring on a slope with dense bushes or trees, the ponding effect is not generally considered because the rainfall flows along the terrain surface. In this study, the area in Fig. 14 marked by a red dotted line was defined as a logging section, and the ponding effect was considered. In the event of rainfall exceeding the saturated permeability coefficient, the daily rainfall penetrating the ground and affecting slope stability was analyzed over time. The boundary conditions were set according to the retaining wall design conditions, as shown in Fig. 15, and the slope stability was examined in connection with seepage analysis for ten days.

Figs. 16-23 show the results of the seepage analysis that applied the daily rainfall conditions shown in Fig. 13. The results could not be presented for all dates. The pore water pressure distribution in the ground, depth of saturation from the surface layer, and safety factor of each slope were determined for days 1, 3, 5, and 10. As rainfall begins, the seepage water flowing along the unsaturated surface depends on the unsaturated permeability coefficient calculated by the soil-water characteristic curve (SWCC, as shown in Table 1). The unsaturated permeability function of weathered soils is the most important hydraulic property governing the flow process. Therefore, various information of the unsaturated permeability function is essential in the

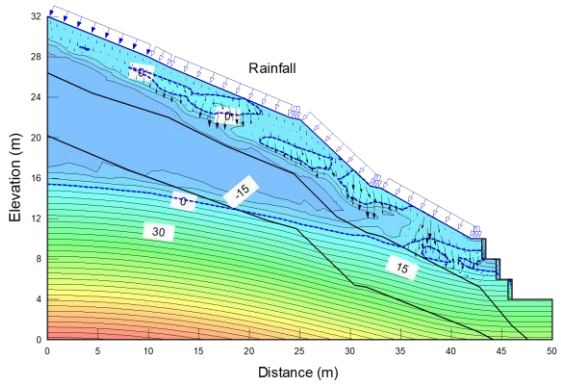

Fig. 18 Contour of pore water pressure (after 3 days)

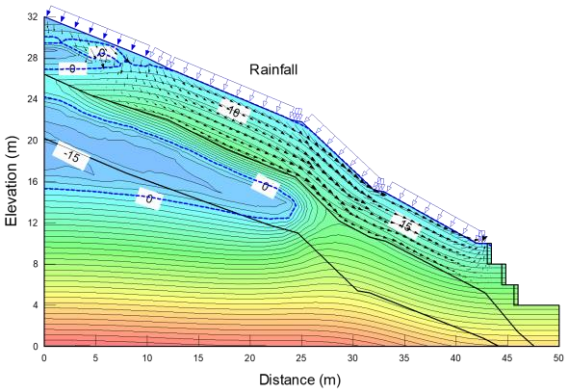

Fig. 22 Contour of pore water pressure (after 10 days)

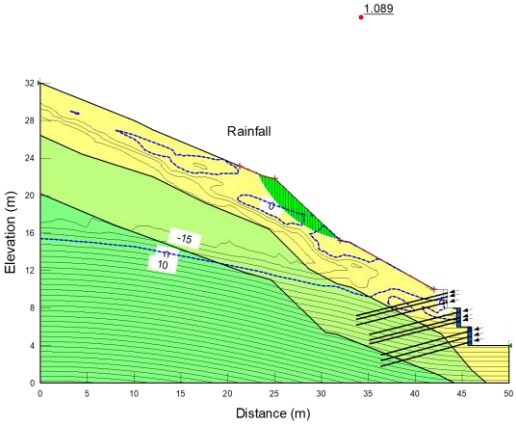

Fig. 19 Safety factor owing to 3 days of rainfall

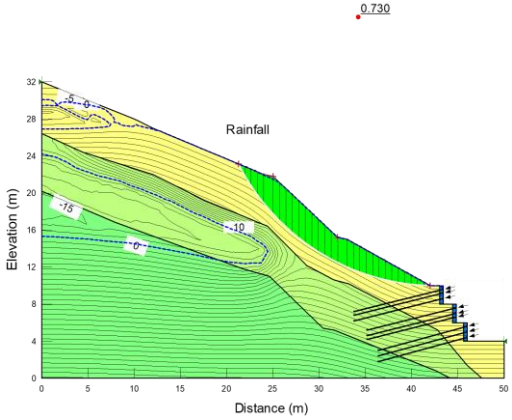

Fig. 23 Safety factor owing to 10 days of rainfall

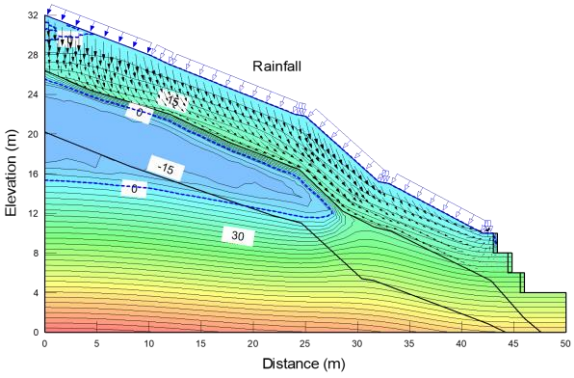

Fig. 20 Contour of pore water pressure (after 5 days)

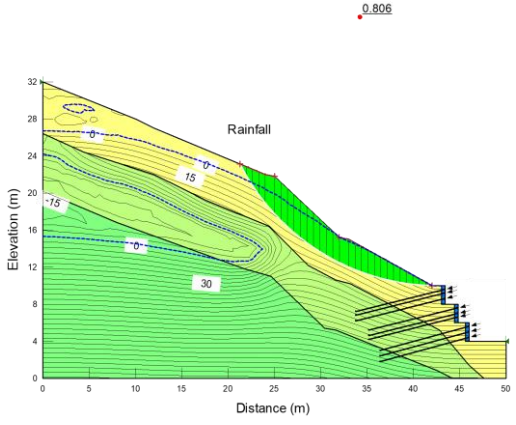

Fig. 21 Safety factor owing to 5 days of rainfall

Table 2 Change on safety factor over 10 days

Date	Rainfall Intensity	Daily Precipitation	Safety Factor
August 22	0	0	1.121
August 23	14.6	57	1.121
August 24	4.3	11.3	1.089
August 25	1.7	2.5	1.089
August 26	29.7	98.6	1.044
August 27	40.4 (failure in analysis)	108.5	0.806
August 28	0.1	0.1	0.798
August 29	0.9	0.9	0.798
August 30	8.9	24	0.754
August 31	53.4 (failure on site)	75.4	0.730

analysis of the flow process in the unsaturated zone. Although the unsaturated permeability function can be directly measured in soil laboratories, a reliable measurement of the permeability function for an unsaturated soil is challenging due to the time-consuming nature and high cost of taking direct measurement. Thus the unsaturated permeability function was estimated and used directly within the software (GeoStudio 2016). As the rainfall was not constant, changes in penetration depth and safety factors did not show constant trends (Lombardi et al., 2017, Pantelidis *et al.* 2020; Rahardjo *et al.* 2009).

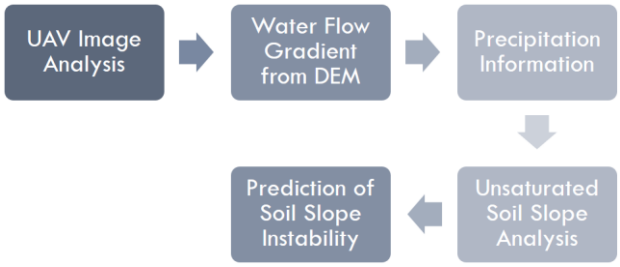

Fig. 24 Methodology for predicting the instability of soil slopes in urban areas

As shown in Eq. (1), the shear strength equation of unsaturated soil utilized in the slope stability analysis was the unsaturated shear strength equation to incorporate the contribution from the negative pore-water pressure. The equation for unsaturated shear strength is as follows (Rahardjo *et al*. 2009). Table 2 summarizes the safety factor of the slope according

$$\tau = c' + (\sigma_n - u_a)\tan\phi' + (u_a - u_w)\tan\phi^b \quad (1)$$

where τ= shear strength of unsaturated soil; c'=effective cohesion; $(\sigma_n - u_a)$=net normal stress; σ_n=total normal stress; u_a=pore-air pressure; ϕ'=effective angle of internal friction; $(u_a - u_w)$ =matric suction; u_w =pore-water pressure; and ϕ^b=angle indicating the rate of increase in shear strength relative to the matric suction. The slope stability analysis using Bishop's simplified method was performed using SLOPE/W software. The pore-water pressures, u_w, obtained from the transient seepage analyses using SEEP/W were exported to SLOPE/W to be incorporated in the slope stability analyses (GeoStudio, 2016).

Table 2 summarizes the safety factor of the slope according to the daily rainfall for ten days. According to the seepage and stability analyses, a failure had already occurred after five days. Although the collapse was found at the site on August 31 (the tenth day), we surmise that the slope failure had already begun in the upper part of the slope after five days. We consider that the surface layer was rapidly saturated because large amounts of water penetrated the ground owing to logging and that the ground strength decreased relatively quickly as the pore water pressure increased and matric suction rapidly decreased (Saseendran and Dodagoudar 2020, Song and Hong 2022, Zhang *et al*. 2015, Zhao *et al*. 2020).

As a result, a flow chart (Fig. 24) showing how UAV data and numerical analyses were used to estimate instability of soil slope in urban areas. This would be a research methodology that can help citizens living in urban areas live safely.

5. Conclusions

In this study, logging areas near the OO High School building in Gwangju, Korea, where heavy rainfall could penetrate were identified using UAV imaging because the cause of slope failure could not be directly confirmed. A numerical analysis was conducted on the relationship between the amount of penetration by heavy rainfall and the section of slope failure by calculating the area and maximum width of the logging areas using UAV imaging. The following conclusions were drawn.

- As many buildings in urban areas, such as schools, hospitals, and apartments, are constructed near the slopes of mountainous areas, aerial photography utilization was examined to prevent property damage and human casualties caused by slope failures. We found that aerial photography could be used to investigate risks and analyze the cause of slope failure.
- The slope map derived from DEM can be used to evaluate risk investigations because it can increase the safety conditions where buildings are exposed to danger resulting from debris flow or the flow of seepage water in urban areas with slopes.
- We confirmed that the instability of a slope can be predicted earlier than the occurrence of an actual collapse by conducting a limited equilibrium analysis in connection with an unsaturated soil seepage analysis by applying the hourly rainfall intensity data obtained from KMA.
- Considering urban areas are exposed to risks resulting from continuous development, such as logging, forest roads, and walking trails, regular preparation of risk maps or raising awareness of environmental changes is required. We determined that imaging techniques can effectively analyze ground disaster risk maps in urban areas.

Acknowledgments

This work was supported by the National Research Foundation of Korea (NRF) grant funded by the Korean government (Ministry of Education) (No. 2020R1I1A-307511011).

References

Al-Mahbashi, A.M., Elkady, T.Y. and Alrefeai, T.O. (2015), "Soil water characteristic curve and improvement in lime treated expansive soil", *Geomech. Eng.*, **8**(5), 687-696. https://doi.org/10.12989/gae.2015.8.5.687.

GeoStudio (2016), version 8.16.5, User's guide, International Ltd., Calgary, Canada.

Gullà, G., Peduto, D., Borrelli, L., Antronico, L. and Fornaro, G. (2017), "Geometric and kinematic characterization of landslides affecting urban areas: the Lungro case study (Calabria, Southern Italy)", *Landslides*, 14(1), 171-188. https://doi.org/10.1007/s10346-015-0676-0.

Kim, J.H., Lim, J.S. and Park, S.W, (2014), "Coupled finite element analysis of partially saturated soil slope stability", *J. Korean Geotech. Soc.*, **30**(4), 35-45.

Kim, Y.S., Kim, J.H., Lee, J.K. and Kim, S.S, (2013). "A study on soil slope stability design considering seepage analysis", *J. Korean Geotech. Soc.*, **29**(1), 135-147.

Kim, T.W., Choi, Y.W. and Kim, J.H. (2021), "Analysis of rainfall seepage and slope stability by mountain slope logging", *Proceedings of the Korean Geotechnical Society Spring National Conference*, March 18~19, Seoul.

KMA (2018), Weather Data Service, Korea Meteorological Administration, https://data.kma.go.kr.

Lombardi, M., Cardarilli, M. and Raspa, G. (2017), "Spatial variability analysis of soil strength to slope stability

assessment", *Geomech. Eng.*, **12**(3), 483-503. https://doi.org/10.12989/gae.2017.12.3.483.

Ministry of Public Safety and Security (MPSS) (2012), "Development of precision Hazard Risk Assessment Methods and Hazard Maps for Landslides and Debris Flows Due to Heavy Rainstorms", Report from the Natural Disaster Reduction Technology Development Group (MPSS-nature-2012-58).

Pantelidis, L, Gravanis, E. and Gkotsis, K.P. (2020), "Stability assessment of soil slopes in three dimensions: The effect of the width of failure and of tension crack", *Geomech. Eng.*, **22**(4), 319-328. https://doi.org/10.12989/gae.2020.22.4.319.

Peduto, D., Santoro, M., Aceto, L., Borrelli, L. and Gulla, G. (2021), "Full integration of geomorphological, geotechnical, A-DInSAR and damage data for detailed geometric-kinematic features of a slow-moving landslide in urban area", *Landslides*, **18**, 807-825. https://doi.org/10.1007/s10346-020-01541-0.

QGIS (2020), QGIS 3.16.3 'Hannover', https://qgis.org/ko/site/forusers/download.htmltqgis.org.

Rahardjo, H., Meilani, I., Leong, E.C. and Rezaur, R.B. (2009), "Shear strength characteristics of a compacted soil under infiltration conditions". *Geomech. Eng.*, **1**(1), 35-52. https://doi.org/10.12989/gae.2009.1.1.035.

Saseendran, R. and Dodagoudar, G.R. (2020), "Reliability analysis of slopes stabilised with piles using response surface method", *Geomech. Eng.*, **21**(6), 513-525. https://doi.org/10.12989/gae.2020.21.6.513.

Song, Y. and Hong, S. (2022), "Infiltration characteristics and hydraulic conductivity of weathered unsaturated soils", *Geomech. Eng.*, **22**(2), 35-52. https://doi.org/10.12989/gae.2020.22.2.153.

Vasuki, Y., Holden, E-J, Kovesi, P. and Micklethwaite, S. (2014), "Semi-automatic mapping of geological structures using UAV-based photogrammetric data: An image analysis approach", *Comput. Geosci.*, **69**(1), 22-32. https://doi.org/10.1016/j.cageo.2014.04.012.

Xiao, Y., Kamat, V.R. and Lee, S. (2018), "Monitoring excavation slope stability using drones", *Proceedings of the ASCE, Construction Research Congress 2018*.

Zhang, G., Tan, J., Zhang, L. and Xiang, Y. (2015), "Linear regression analysis for factors influencing displacement of high-filled embankment slopes", *Geomech. Eng.*, **8**(4), 511-521. https://doi.org/10.12989/gae.2015.8.4.511.

Zhao, L., Huang, Y., Xiong, M. and Ye, G. (2020), "Reliability and risk assessment for rainfall-induced slope failure in spatially variable soils", *Geomech. Eng.*, **22**(3), 207-217. https://doi.org/10.12989/gae.2020.22.3.207.